Characterization of a Transient Covalent Adduct Formed during Dimethylarginine Dimethylaminohydrolase Catalysis†

Everett M. Stone,‡ Maria D. Person,§ Nicholas J. Costello,|| and Walter Fast*,‡,⊥

Divisions of Medicinal Chemistry and Pharmacology and Toxicology, College of Pharmacy, Graduate Programs in Biochemistry and Cell and Molecular Biology, and The Center for Molecular and Cellular Toxicology, The University of Texas, Austin, Texas 78712

Received December 9, 2004; Revised Manuscript Received February 18, 2005

ABSTRACT: Dimethylarginine dimethylaminohydrolase (DDAH) regulates the concentrations of human endogenous inhibitors of nitric oxide synthase, N^{ω}-methyl-L-arginine (NMMA), and asymmetric N^{ω},N^{ω}-dimethyl-L-arginine (ADMA). Pharmacological regulation of nitric oxide synthesis is an important goal, but the catalytic mechanism of DDAH remains largely unexplored. A DDAH from *Pseudomonas aeruginosa* was cloned, and asymmetrically methylated arginine analogues were shown to be the preferred substrates, with ADMA displaying a slightly higher k_{cat}/K_M value than NMMA. DDAH is similar to members of a larger superfamily of guanidino-modifying enzymes, some of which have been shown to use an *S*-alkylthiouronium intermediate during catalysis. No covalent intermediates were found to accumulate during steady-state turnover reactions of DDAH with NMMA or ADMA. However, identification of a new substrate with an activated leaving group, *S*-methyl-L-thiocitrulline (SMTC), enabled acid trapping and ESI-MS characterization of a transient covalent adduct with a mass of 158 ± 10 Da that accumulates during steady-state turnover. Subsequent trapping, proteolysis, peptide mapping and fragmentation by mass spectrometry, and site-directed mutagenesis demonstrated that this covalent adduct was attached to an active site residue and implicates Cys249 as the catalytic nucleophile required for intermediate formation. The use of covalent catalysis clearly links DDAH to this superfamily of enzymes and suggests that an *S*-alkylthiouronium intermediate may be a conserved feature in their mechanisms.

Nitric oxide (•NO)[1] acts as a biological signaling molecule with numerous functions in healthy human physiology, including neuronal signaling, regulation of blood pressure, and the immune response (*1*). Considering the reactive nature of this radical, biological systems must guard against the destructive properties of excess •NO production, especially in brain tissue which is particularly sensitive to oxidative damage (*2*). The pathogenic effects of •NO have been implicated in cerebral ischemic damage during stroke and in tumor progression as well as a variety of other disease states (*1, 3*). Not surprisingly, neuronal •NO synthase activity is regulated by many mechanisms, including endogenous pools of N^{ω}-methyl-L-arginine (NMMA, **1**) and asymmetric N^{ω},N^{ω}-dimethyl-L-arginine (ADMA, **2**), that inhibit •NO synthase and limit •NO production in vivo (*1*). The concentrations of these endogenous inhibitors are, in turn, regulated by the enzyme dimethylargininase (also called dimethylarginine dimethylaminohydrolase or DDAH, EC 3.5.3.18), which hydrolyzes these compounds (*4*). For example, in a tissue sample of rat aorta, selective inhibition of DDAH increases levels of methylarginines, thereby inhibiting •NO synthase, lowering levels of •NO production, and causing blood vessel contraction (*5*). Studies with cultured endothelial cells and with transgenic mice expressing human DDAH have also illustrated the ability of DDAH to control endogenous •NO biosynthesis (*6*). Despite its importance, only limited studies (*7*−*11*) on the catalytic mechanism of DDAH have been reported.

† This research was supported by the American Heart Association (SDG 0435178N), the Robert A. Welch Foundation (F-1572), and a University Co-operative Society Undergraduate Research Fellowship to N.J.C. from the University of Texas. Mass spectra were acquired in the CRED Analytical Core supported by NIEHS Grant ES07784.

* To whom correspondence should be addressed: College of Pharmacy, PHAR-MED CHEM, The University of Texas, 1 University Station, A1935, Austin, TX 78712. Phone: (512) 232-4000. Fax: (512) 232-2606. E-mail: WaltFast@mail.utexas.edu.

‡ Graduate Program in Cell and Molecular Biology.

§ Division of Pharmacology and Toxicology, College of Pharmacy.

|| University of Texas at Austin.

⊥ Division of Medicinal Chemistry, College of Pharmacy, Graduate Program in Biochemistry, and The Center for Molecular and Cellular Toxicology.

[1] Abbreviations: •NO, nitric oxide; DDAH, dimethylarginine dimethylaminohydrolase; *Pa*, *Pseudomonas aeruginosa*; NMMA, N^{ω}-methyl-L-arginine; ADMA, asymmetric N^{ω},N^{ω}-dimethyl-L-arginine; SMTC, *S*-methyl-L-thiocitrulline; ESI-MS, electrospray ionization mass spectrometry; MALDI-TOF, matrix-assisted laser desorption ionization time-of-flight; PSD, post-source decay; αGlc, α-N-gluconoylation; IMO, 1-(iminomethyl)-L-ornithine; LB, Luria−Bertani; PCR, polymerase chain reaction; SDS−PAGE, sodium dodecyl sulfate−polyacrylamide gel electrophoresis; OD_{600}, optical density at 600 nm; ICP-MS, inductively coupled plasma mass spectrometry; ORF, open reading frame.

10.1021/bi047407r CCC: $30.25
Published on Web 04/16/2005

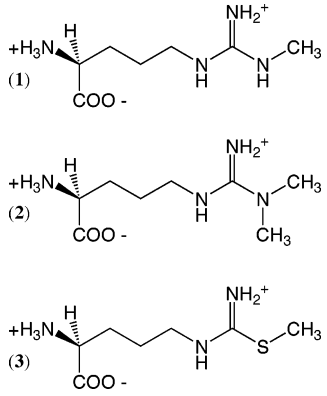

A recent crystal structure of DDAH from *Pseudomonas aeruginosa* (*Pa* DDAH) represents an important advance and reveals an overall α/β propeller structure with 5-fold pseudosymmetry that binds the substrate at the center of the propeller and is capped by a long surface loop (*8*). The catalytic residues responsible for hydrolysis are located deeper within DDAH where the guanidino group of the substrate binds. There are no reported structures for the two known human DDAH isoforms (DDAH-1 and DDAH-2), but they are overall 23−29% identical to *Pa* DDAH in terms of amino acids, and the active-site residues are much more stringently conserved (*12*). Amino acid sequence, structural alignments, and similarities between reaction chemistry suggest that DDAH belongs to a larger superfamily of guanidino-modifying enzymes including arginine deiminase, arginine:glycine amidinotransferase, arginine:inosamine-phosphate amidinotransferase, and peptidylarginine deiminase (*13*). Two of the other superfamily members have been shown to use covalent catalysis in their reaction mechanisms, but the reaction mechanism of DDAH has not been well characterized. In this study, we used alternative substrates, steady-state kinetics, and mass spectrometry to investigate the specificity and catalytic mechanism of DDAH.

MATERIALS AND METHODS

Construction of an Expression Vector for Pa DDAH. The coding region for *Pa* DDAH (Protein GI:53727549) was amplified from *P. aeruginosa* genomic DNA (ATCC 470850) using two specific end primers: 5′-CAGGATCCCATATGTTCAAGCACATCATCGCTCG-3′ and 5′-CGGAATTCTCAGAAGCGCAGCGACATG-3′ (Sigma-GENOSYS, The Woodlands, TX). The forward primer contains an *Nde*I restriction site (underlined) followed by 20 bases corresponding to the coding sequence of the DDAH gene. The reverse primer contains an *Eco*RI restriction site (underlined) followed by 16 bases corresponding to the gene coding sequence. Amplification of the *Pa* DDAH gene was carried out by PCR using an MJ Research (Waltham, MA) PTC 200 thermocycler, along with the aforementioned primers, genomic DNA, dNTPs (New England Biolabs, Beverly, MA), and Triplemaster PCR reagents (Eppendorf, Westbury, NY) following a temperature program: 95 °C for 5 min, followed by 30 cycles of 95 °C for 30 s, 52 °C for 30 s, and 72 °C for 1 min, followed by a 3 min hold at 72 °C. The PCR-amplified *Pa* DDAH coding sequence was then ligated into a pGEM-T vector (Promega, Madison, WI) and transformed into *Escherichia coli* DH5αE cells. The resulting plasmid (pTpaoDDAH) was isolated, and the insert was sequenced to ensure that there were no undesired mutations. The pTpaoDDAH plasmid and the pET-28a expression vector were subsequently digested with *Nde*I and *Eco*RI restriction enzymes followed by gel purification and ligation of the digested *Pa* DDAH coding sequence into the multiple cloning site of pET-28a. The resulting plasmid (designated pETpaDH) was transformed into *E. coli* DH5α cells for purification and sequencing of the insert.

Construction of an Expression Vector for C249S DDAH. An oligonucleotide, 5′-CGGAATTCTCAGAAGCGCAGCGAGCAggaACTGACG-3′ (Sigma-GENOSYS), that contained an *Eco*RI restriction site (underlined) and a mutant codon (lowercase) was designed to introduce a mutation encoding C249S at the end of the DDAH sequence. Because the desired mutation was near the 3′ end of the *Pa* DDAH gene, only one PCR was required, using the mutant reverse primer and forward primer described above with the aforementioned reaction conditions. After Qiaquick (Qiagen, Valencia, CA) purification of the C249S PCR product, this insert and a pET-28a expression vector were digested with *Nde*I and *Eco*RI, Qiaquick purified (Qiagen), and ligated together using T4 DNA ligase (Fischer, Pittsburgh, PA). The resulting plasmid (pET-DH-C249S) was concentrated by pellet paint precipitation (Novagen, San Diego, CA) and transformed into *E. coli* DH5αE cells for plasmid amplification and purification. DNA sequencing of the coding sequence of the C249S insert indicated that there were no undesired mutations.

Overexpression and Purification of Wild-Type and C249S Pa DDAH. For expression of wild-type and C249S *Pa* DDAH, the expression plasmids were first transformed into *E. coli* BL21(DE3) cells. Typically, overexpression of *Pa* DDAH was carried out by inoculating 1 L of LB medium containing 30 μg/mL kanamycin with 10 mL of inoculant from a saturated overnight culture and shaking at 37 °C. IPTG was added to a final concentration of 0.5 mM when the expression culture reached an OD_{600} of 0.5, and expression was continued for an additional 4 h. Cells were then harvested by centrifugation and stored at −20 °C. Frozen cell pellets were resuspended in pET lysis buffer [10 mM NaH_2PO_4 buffer, 300 mM NaCl, and 10 mM imidazole (pH 8.0)] at 40 mL of buffer/L of culture. Cell suspensions were sonicated on ice for 2 min with 15 s burst/rest cycles followed by centrifugation at 23500*g* for 20 min. Approximately 15 mL of supernatant was then loaded directly onto an 8 mL Ni−NTA affinity resin column (Qiagen) and washed with 10 column volumes of lysis buffer (see above), followed by 7 column volumes of 50 mM NaH_2PO_4 buffer, 300 mM NaCl, and 20 mM imidazole (pH 8.0), and finally eluted with 50 mM NaH_2PO_4 buffer, 300 mM NaCl, and 250 mM imidazole (pH 8.0). Fractions (3 mL) were characterized by activity and SDS−PAGE. The wild-type *Pa* DDAH did not require additional purification, but the C249S mutant was further purified by loading fractions containing the desired protein onto a DEAE ion-exchange column. This column was washed with 20 mM Tris-HCl buffer (pH 8.0), and then purified protein was eluted stepwise by the addition of a mixture containing 75% of 20 mM Tris-HCl buffer (pH 8.0) and 25% of 20 mM Tris-HCl buffer and 1 M NaCl (pH 8.0). Fractions were characterized by SDS−PAGE, and those containing purified protein were pooled. To remove any extraneously bound metal ions, purified proteins were

dialyzed overnight at 4 °C in 4 L of 2 mM 1,10-phenanthroline and 100 mM KCl (pH 7), followed by two 4 h dialyses composed of 4 L each of Chelex-100-treated (Bio-Rad, Hercules, CA) 10 mM MES and 100 mM KCl at pH 6.2 and 4 °C. The final purification products were made 10% in glycerol and stored in aliquots at −80 °C after being flash-frozen in liquid N_2.

Characterization of Pa DDAH. The first 15 N-terminal residues of purified wild-type *Pa* DDAH were sequenced by Edman degradation at the Protein Facility (Institute for Cellular and Molecular Biology, The University of Texas). To determine the final metal content, a protein sample (79 μM) and associated dialysis buffer were analyzed by inductively-coupled plasma mass spectrometry (ICP-MS, Department of Geological Sciences, The University of Texas) to quantify the protein's zinc content by subtracting the concentration of zinc found in dialysis buffer from the zinc concentration of the final protein sample and dividing by the protein concentration. To determine protein concentrations, an extinction coefficient was calculated for *Pa* DDAH on the basis of the amino acid sequence (http://workbench.sdsc.edu/) (*14*). All protein concentrations for DDAH were calculated on the basis of the calculated ϵ_{280} of 17 210 M^{-1} cm^{-1} in a final buffer concentration of 6 M guanidinium hydrochloride and 20 mM phosphate buffer (pH 6.5).

Mass Spectrum Analysis of Products Formed in the DDAH Reaction. Because the standard colorimetric assay used for citrulline (*15*) detects ureido groups and is not specific for citrulline formation (*16*), mass spectrometry was used to establish the reaction products of *Pa* DDAH. A Sephadex G-10 spin column was used to exchange a sample of enzyme into 25 mM ammonium bicarbonate buffer (pH 7). An amount (1 μmol) of ADMA was then incubated overnight with 375 pmol of *Pa* DDAH in 25 mM ammonium bicarbonate buffer (pH 7). The subsequent reaction products were analyzed by MALDI-TOF. Two control samples, one lacking enzyme and one lacking substrate, were also analyzed on an Applied Biosystems (Foster City, CA) Voyager-DE PRO mass spectrometer using α-cyano-4-hydroxycinnamic acid as the matrix as previously described (*17*).

Steady-State Kinetic Studies. Using a slightly modified published protocol (*18*) that detects formation of a ureido group, the steady-state catalytic rate constants of *Pa* DDAH were determined for hydrolysis of various compounds, including creatine, creatinine, argininosuccinate, guanidinoacetate, L-arginine, L-homoarginine, L-canavanine, N^{ω}-amino-L-arginine, N^{ω}-hydroxy-L-arginine, N^{ω}-methyl-L-arginine (NMMA, **1**), N^{ω},N^{ω}-dimethyl-L-arginine (ADMA, **2**), and *S*-methyl-L-thiocitrulline (SMTC, **3**) (Sigma-Aldrich Chemical Co., St. Louis, MO). Typically, substrate concentrations ranging from 78 μM to 10 mM were prepared by serial dilution in an assay buffer consisting of 100 mM Na_2HPO_4 buffer (pH 6.2). Substrate aliquots of 200 μL were placed in 1.5 mL microcentrifuge tubes to which 5 μL of a 79 μM enzyme stock was added. Most reactions were carried out at 25 °C for 1 min, and then stopped by addition of 10 μL of 6 N trichloroacetic acid. Control reactions showed that citrulline production under these conditions is linear for more than 5 min. Slower substrates such as L-arginine were assayed at 25 °C for longer periods of time (2 h) with increased enzyme concentrations (4.5 nM). Compounds that displayed no turnover were further tested at 25 °C for activity by incubating each compound (5 mM) with a higher concentration of enzyme (6 μM) for 1 h. A control reaction without the enzyme was also performed at each substrate concentration, enabling background citrulline levels to be subtracted. A series of standards for quantifying final citrulline concentrations was prepared by serially diluting citrulline to a final concentration range of 0−313 μM in 100 mM Na_2HPO_4 buffer (pH 6.2) and aliquoting these samples in 200 μL portions in 1.5 mL microcentrifuge tubes. To the citrulline standards, enzyme reaction mixtures, and controls was added 1 mL of freshly prepared color-developing reagent (*18*), and the tubes were placed in a boiling water bath for 15 min and then cooled for 10 min at 25 °C. The absorbance at 540.5 nm was measured for each sample using a Cary 50 UV−vis spectrophotometer (Varian Inc., Walnut Creek, CA) and then converted into citrulline concentrations by using a standard curve. The resulting data, after background subtraction, were fit directly to the Michaelis−Menten equation using KaleidaGraph (Synergy Software, Reading, PA). All reactions were carried out in at least triplicate. Activity tests for the C249S mutant were also performed using 10 mM substrates (**1**−**3**) for 1 h at 37 °C to maximize the chance of detecting any citrulline that might be formed.

Mass Spectrum Analysis of Covalently Modified Pa DDAH. To characterize a covalent enzyme−substrate intermediate that might accumulate during steady-state reactions, incubations of **1**−**3** and DDAH were quenched with acid during turnover. Samples were typically prepared by incubating 20−60 μM enzyme and 10−45 mM substrate in 10 mM MES buffer, 100 mM KCl, and 10% (v/v) glycerol (pH 6.2) at 25 °C, followed by quenching with 1 M trifluoroacetic acid to a final concentration of 83 mM after reaction for 0, 1, 5, and 30 min. A control lacking substrate was included for every reaction. Samples were then desalted on a protein trap (Protein MicroTrap, Michrom, Auburn, CA) and analyzed by electrospray ionization mass spectrometry (ESI-MS) on a ThermoFinnigan LCQ (San Jose, CA) ion trap mass spectrometer as described previously (*19*) using a 10 min 5 to 95% B gradient delivered by a Michrom Magic 2002 HPLC system.

Identification of Covalently Modified Peptide. Steady-state reaction mixtures of *Pa* DDAH and SMTC (**3**) were prepared and the reactions quenched with acid as described above. A Sephadex G-10 spin column was then used to exchange these reaction mixtures into 50 mM ammonium acetate buffer (pH 4) where the covalent adduct is stable (data not shown) and where an acid stable protease would be active. The resulting product was subsequently digested with Glu-C endoproteinase (Roche, Indianapolis, IN) in a 20:1 (w/w) ratio for 18 h at room temperature. Digestion products were analyzed using MALDI-TOF and MALDI-PSD on an Applied Biosystems Voyager-DE PRO system using α-cyano-4-hydroxycinnamic acid as the matrix as previously described (*17*). Theoretical digest masses were calculated with MS-Digest in the Protein Prospector suite using two missed cleavages (*20*).

RESULTS

Expression and Characterization of Wild-Type and C249S Pa DDAH. The *Pa* DDAH coding sequence was amplified from genomic DNA and cloned into a pET-28a expression

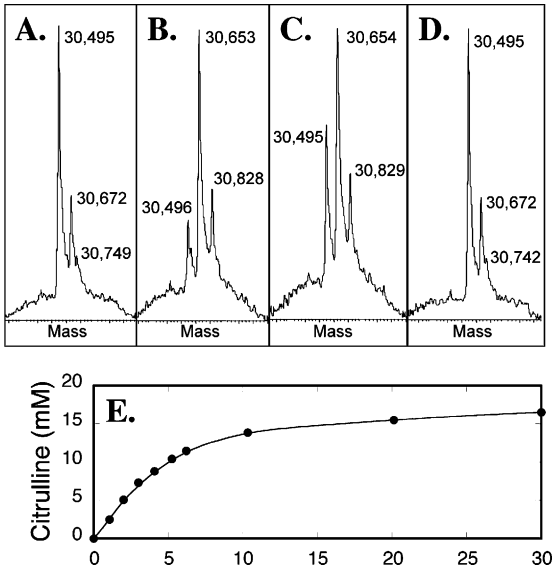

FIGURE 1: Deconvoluted ESI-MS of quenched DDAH reactions with *S*-methyl-L-thiocitrulline (SMTC, **3**). Reactions are acid-quenched before (A) and after addition of **3** with subsequent turnover for (B) 1, (C) 5, and (D) 30 min. The minor peaks that consistently contain a 178 Da adduct throughout the reaction reflect a fraction of the enzyme that is α-N-gluconoylated during expression (*21*). (E) A progress curve showing hydrolysis of **3** (20 mM) to citrulline under the same conditions that were used for the trapping experiments in panels A−D indicates that the fastest rate of hydrolysis corresponds with the sample containing the most 157 Da adduct and that, after turnover is finished, the enzyme does not contain this 157 Da adduct.

vector without any undesired mutations. The resulting N-terminal His_6-tagged protein was overproduced in BL21-(DE3) *E. coli*, and a single affinity chromatography step resulted in homogeneous wild-type *Pa* DDAH (>98% homogeneous) as assessed by SDS−PAGE. Characterization of the purified protein by ESI-MS showed a major peak at 30 495 ± 10 Da, which matches (within error) the mass calculated from the amino acid sequence (30 503 Da) of His_6-tagged *Pa* DDAH when the N-terminal methionine residue had been removed (Figure 1A). The first 15 amino acids of the purified protein were identified by N-terminal sequencing to give a GSSHHHHHHSSGLVP sequence, confirming that the N-terminal methionine had been removed. ESI-MS of protein samples gauged to be homogeneous by SDS−PAGE did reveal a minor peak that carries an additional 177 ± 10 Da adduct and a small peak indicating an additional 254 ± 10 Da adduct, both of which are consistent with a minor fraction of the purified DDAH carrying a nonenzymatic modification at the N-terminus from α-gluconoylation and α-6-phosphogluconoylation, respectively, both of which have previously been characterized in other recombinant proteins containing polyhistidine tags (*21*). The total amount of gluconoylation varied among enzyme preparations, but was always only a minor component. The modified and unmodified N-terminal His_6 tags were not removed for these tests because the crystal structure of this enzyme places the N-terminus distant from both the active site (*8*) and the dimer interface (*22*), the His_6 fusion was previously shown to be active (*23*), and short N-terminal extensions of other DDAH isoforms do not significantly affect their kinetics (*24*). Unlike the wild-type protein, the C249S mutant required an additional purification step. Hence, ion-exchange chromatography followed the initial affinity column and resulted in >95% purity as assessed by SDS−PAGE. Because zinc has been shown to inhibit the activity of bovine brain DDAH (*11*, *25*), chelation and dialysis steps were carried out at the end of the purification to remove any remaining zinc ions. For both the wild type and the C249S mutant, less than 0.001 equiv of zinc was found in the final purified proteins.

Table 1: Steady-State Rate Constants for DDAH-Catalyzed Hydrolysis of Substrates, Ranked by Increasing k_{cat}/K_M Values

substrate	k_{cat} (min^{-1})	K_M (μM)	k_{cat}/K_M (min^{-1} mM^{-1})
L-arginine[a]	0.10 ± 0.02	940 ± 50	0.11 ± 0.03
N^{ω}-amino-L-arginine[a]	7.2 ± 0.1	1110 ± 60	6.5 ± 0.4
N^{ω}-hydroxy-L-arginine[a]	20 ± 2	2300 ± 400	9 ± 2
NMMA (**1**), rat DDAH[b]	5.6	360 ± 10	16
NMMA (**1**)[a]	18.6 ± 0.6	670 ± 60	28 ± 3
ADMA (**2**), rat DDAH[b]	9.2	180 ± 10	51
ADMA (**2**)[a]	33.6 ± 0.6	310 ± 20	108 ± 9
SMTC (**3**)[a]	50.4 ± 0.6	143 ± 5	350 ± 20

[a] Reactions are carried out with *Pa* DDAH at 25 °C and pH 6.2. [b] Values are from ref *7*, and were determined with rat kidney DDAH at 37 °C and pH 6.5.

Mass Spectral Analysis of Substrate Digestion Products. The substrate ADMA was completely hydrolyzed by purified DDAH, and the reaction products were analyzed by MALDI-TOF. A control reaction, lacking enzyme, was used to determine the mass of unhydrolyzed ADMA: $M{\cdot}H^+_{obs}$, 203.1 ± 0.1 Da; $M{\cdot}H^+_{calc}$, 203.14 Da. MALDI-TOF of reaction mixtures in which ADMA was incubated with purified DDAH showed a loss of this 203.1 Da peak and the appearance of two new peaks at 46.0 ± 0.1 and 176.1 ± 0.1 Da, corresponding to the calculated masses of dimethylamine ($M{\cdot}H^+_{calc}$, 46.06) and citrulline ($M{\cdot}H^+_{calc}$, 176.10).

Determining the Steady-State Kinetic Constants. An established discontinuous assay for citrulline production (*18*) was used to follow any hydrolysis reactions observed with varying concentrations of different compounds as catalyzed by the purified wild-type *Pa* DDAH (Table 1). This enzyme was shown to prefer ADMA over NMMA (indicated by a 3.9-fold increase in k_{cat}/K_M), but the artificial substrate SMTC had the highest k_{cat} (1.5-fold increase) and the lowest K_M (2.2-fold decrease) of all of the substrates that were tested. Substrate inhibition was observed with NMMA, ADMA, N^{ω}-hydroxy-L-arginine, and N^{ω}-amino-L-arginine at concentrations above 10 mM, but SMTC did not show any substrate inhibition at concentrations up to 40 mM (data not shown). Further experiments will be required to determine the mechanism of substrate inhibition, so concentrations of <10 mM were typically used for these studies.

Less active substrates include N^{ω}-hydroxy-L-arginine, N^{ω}-amino-L-arginine, and L-arginine that have k_{cat}/K_M values 8-, 17-, and 1000-fold lower, respectively, than that of ADMA. Creatine, creatinine, argininosuccinate, guanidinoacetate, L-homoarginine, and L-canavanine were not good substrates, exhibiting either no activity or less activity than L-arginine. We were unable to detect any activity for the C249S mutant-catalyzed hydrolysis of compounds **1**−**3** under the conditions described above, indicating that the k_{cat} of this mutant must be lowered by at least 5 orders of magnitude.

Mass Spectrometry of Acid-Quenched Steady-State Reactions. To obtain evidence for a transient covalent adduct, reactions were acid-quenched at various time points before,

during, and after turnover and then analyzed by ESI-MS. The deconvoluted mass spectrum of a control reaction, quenched before addition of substrate, results in a major peak at 30 495 ± 10 Da (Figure 1A) matching that of unmodified *Pa* DDAH (see above). The minor peak seen at 30 672 Da is assigned to the fraction of DDAH with α-gluconoylation at the N-terminus. Analysis of a steady-state reaction between SMTC and DDAH that was quenched after 1 min of turnover clearly shows that the major peak shifts 158 Da higher to 30 653 ± 10 Da, with only a minor amount of the unmodified 30 496 Da peak remaining (Figure 1B). The small peak due to the fraction of enzyme that is α-N-gluconoylated also shifts an equivalent amount (156 ± 10 Da) and maintains a similar ratio to the major peak throughout the reaction. A reaction quenched after 5 min of turnover (Figure 1C) results in essentially the same peaks that are seen in the 1 min sample, but the relative peak heights of the major peak (30 654 Da) and the unmodified enzyme peak (30 495 Da) have changed, showing an increase in the unmodified enzyme peak after reaction for 5 min. Finally, after a 30 min reaction (Figure 1D), the spectrum does not show any peaks different from those observed in the starting sample (Figure 1A).

The progress curve for *Pa* DDAH-catalyzed conversion of SMTC (20 mM) to citrulline was determined for a reaction using the same conditions that were used for preparing the ESI-MS samples described above (Figure 1E). It should be noted that these experiments involve much more enzyme than is normally used when measuring initial rates. Citrulline is produced at the highest rate during the first 1 min, which corresponds to the ESI-MS spectrum showing the largest 158 ± 10 Da adduct peak (Figure 1B). After the reaction has progressed for 5 min, the rate of citrulline production is slowed, most likely due to product inhibition (*26*) under these conditions, and corresponds to the ESI-MS spectrum in which less of the 159 ± 10 Da adduct is seen relative to the unmodified enzyme (Figure 1C). Finally, after 30 min, the reaction slows because the conversion of SMTC to citrulline is nearly complete, and this corresponds to the ESI-MS spectrum (Figure 1D) that is nearly identical to that taken before the reaction was started (Figure 1A). In short, a covalent adduct of 158 ± 10 Da transiently appears during *Pa* DDAH-catalyzed turnover of SMTC. The ratio of this adduct to the unmodified enzyme is the largest during the fastest initial hydrolysis rates, decreases when less enzyme is available to react with the substrate (probably due to product inhibition), and disappears when the conversion is complete.

Despite its lack of activity, the C249S mutant was also tested for possible formation of a covalent adduct upon incubation with SMTC. ESI-MS of the quenched incubations only showed one major peak at 30 481 ± 10 Da, consistent with a calculated mass of 30 487 Da for the C249S mutant after removal of the N-terminal methionine.

Identification of the Covalently Modified Peptide. To determine both the residue that is transiently modified and a more precise mass of the covalent adduct, an acid-trapped reaction mixture containing both the unmodified enzyme and the enzyme containing the 158 Da adduct was digested by Glu-C endoproteinase and the resulting peptides were detected by using MALDI-TOF in both linear and reflectron modes. The theoretical digest peptide molecular masses were compared to the observed MS data, and 24 different peptides covering 74% of the total sequence were successfully detected, including peptides containing active site residues Cys249, His162, Glu114, and Thr165 (Table 2). An N-terminal peptide was detected and corresponds to the mass of the first 52 residues without the N-terminal methionine, again showing removal of the N-terminal methionine during expression and purification of His_6-tagged *Pa* DDAH. A minor peak corresponding to this same N-terminal peptide but with an additional 178 ± 1 Da was also observed, consistent with a small amount of DDAH undergoing nonenzymatic N-terminal α-gluconoylation during expression as reported with other recombinant proteins (*21*). A small amount of a 258 Da adduct to this peptide was also observed (data not shown) in our samples, consistent with the presence of a very minor fraction of an α-*N*-6-phosphocluconoyl modification usually found in small amounts when this nonenzymatic gluconoylation occurs during overexpression (*21*).

Table 2: Summary of Proteolytic Cleavage of DDAH with Glu-C Endoproteinase[a]

DDAH sequence positions plus leader (−18 to 0)	calculated average peptide mass (Da)	observed peptide mass (Da)[b]
−18 to 33	5657.4	5658.1
−18 to 33 + αGlc[c]	5835.5	5835.8
34−56	2627.0	
57−65	1096.2	
66−83	1903.2	
84−88	604.6	
89 and 90	249.2	
91−93	374.4	
94	148.1	
95−105	1323.7[e]	1323.7[e]
95−114	2277.6	2277.4
95−129	3914.5	3914.4
106−108	417.5	
109−114	573.6	
115−129	1655.9	1655.7
115−146	3469.0	3468.7
130−136	748.8	
130−146	1832.1	1831.9
130−158	3095.6	
137−146	1101.6[e]	1101.6[e]
147−158	1281.7[e]	1281.7[e]
147−171	2749.3	2749.0
147−180	3669.3	3669.0
147−186	4357.1	4356.8
159−171	1485.8	1485.8
159−180	2405.8	2405.7
159−186	3093.6	3094.0
187−194	1026.1	
195−197	358.4	
198−210	1528.6	1528.9
200−210	1270.4	
211−223	1546.8	1546.7
211−234	2846.4	2846.3
211−239	3378.0	3377.7
224−234	1317.8[e]	1317.8[e]
235−254	2264.6	2264.3
240−254	1733.1	1733.1
240−254 + IMO[d]	1890.2	1890.3

[a] Comparison of calculated peptide masses (MS-Digest in Protein Prospector) with experimental results by MALDI-TOF for digestion with up to two missed cleavages. Amino acid numbering is assigned to match that of Protein Data Bank entry 1H70 (*8*). [b] Mass accuracy is 200 ppm. [c] αGlc stands for N-terminal α-gluconoylation (*21*). [d] IMO stands for the 1-(iminomethyl)-L-ornithine fragment of the covalent adduct (Figure 2). [e] Monoisotopic mass.

Table 3: Summary of Ions Observed in MALDI-PSD Fragmentation Spectrum[a]

1733 Da peptide		1890 Da peptide	
ion	*m*/*z*	ion	*m*/*z*
R	70	R	70
V	72	V	72
K	84	K	84
I/L	86	I/L	86
R	87	R	87
R	112	R	112
	115		115
K	129	K	129
Y	136	Y	136
b_2	303	b_2	
b_5	676	b_5	676
			993
		y_{10}*-IMO-S	1022
y_{10}	1058	y_{10}*-IMO	1056
	1527		
		y_{14}*-IMO-S	1535
y_{14}	1568		
		MH^+-H_2O-IMO-S	1682
		MH^+-IMO-S	1700
MH^+-H_2O	1716	MH^+-H_2O-IMO	1716
MH^+	1733	MH^+-IMO	1733

[a] IMO stands for the 1-(iminomethyl)-L-ornithine fragment of the covalent adduct (Figure 2). Mass accuracy is 1500 ppm.

Importantly for the detection of a covalent adduct, the linear MALDI spectrum of the digestion mixture shows a peptide at *m*/*z* 1732.9, corresponding to the average mass of the C-terminal DDAH peptide following Glu-C cleavage ($_{240}$YRKIDGGVSCMSLRF$_{254}$). This C-terminal peptide contains the active site Cys249 residue. The same spectrum also shows a peptide at *m*/*z* 1890.2, which does not correspond to the mass of any predicted DDAH Glu-C cleavage peptide, but is 157.3 ± 0.4 Da higher than the DDAH C-terminal peptide mass. This postulated adduct is consistent with the 158 ± 10 Da adduct found when the undigested protein was analyzed by ESI-MS. The peptide at *m*/*z* 1890 is not seen in the MALDI reflectron spectrum, demonstrating that it contains a bond that readily fragments after ionization. No mass increase was found for any of the 23 other peptides found in the digest. Comparison of the C-terminal adduct to the ESI-MS results of the intact protein indicates that there is just a single modification, excluding the missing peptides in the digest as sites for multiple attachments.

To identify the modified residue, ions from the MALDI post source decay (PSD) fragmentation spectra of both the native C-terminal peptide at *m*/*z* 1733 and the modified peptide at *m*/*z* 1890 were compared (Table 3). Immonium ions, b ions, and y ions (see ref *27* for nomenclature) from each parent confirm that both peptides are derived from the same amino acid sequence. The primary fragments for the *m*/*z* 1733 peptide are b_5 and y_{10} ions produced by fragmentation after an Asp residue. The *m*/*z* 1890 peptide undergoes a dominant fragmentation involving neutral loss of 157 and 190 Da to produce the *m*/*z* 1733 and 1700 fragments, respectively, consistent with fragmentation on either side of a sulfur atom (Figure 2). The sum of these observations shows that modification occurs at the only cysteine residue found within this peptide, Cys249.

DISCUSSION

DDAH isoforms play a significant role in regulating the concentration of human endogenous •NO synthase inhibitors,

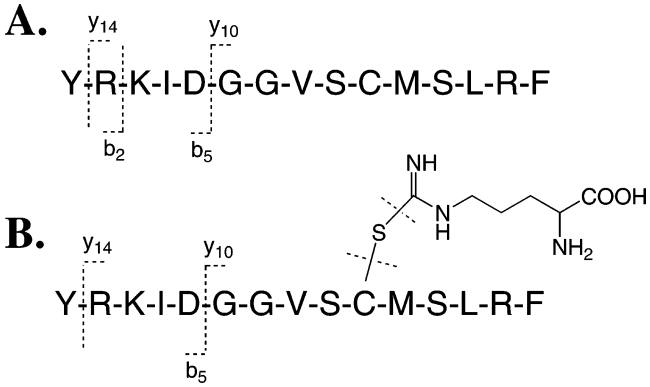

FIGURE 2: Fragmentation patterns from MALDI-PSD. (A) The 1733 Da peptide shows y_{14}, y_{10}, b_2, and b_5 fragments. (B) The 1890 Da peptide shows the same b_5 fragment, but y_{14} and y_{10} also contain an additional adduct. Fragmentation on either side of a sulfur atom implicates a cysteine side chain as the point of attachment.

N^{ω}-methyl-L-arginine (NMMA) and asymmetric N^{ω},N^{ω}-dimethyl-L-arginine (ADMA), by metabolizing these inhibitors to citrulline and the corresponding alkylamine (*4*). Determining the catalytic reaction mechanism of this enzyme will be helpful in understanding its role in the biological regulation of •NO synthesis and in designing specific inhibitors with therapeutic potential. However, there have only been limited studies (*7*−*11*) on the reaction mechanism of this enzyme.

On the basis of its sequence (*13*) and structure (*8*), DDAH has been assigned to a superfamily of guanidino-modifying enzymes. Two of the other enzymes in this superfamily that have been studied in more detail have been shown to use a covalent intermediate in their reaction mechanisms: L-arginine:glycine amidinotransferase (*28*, *29*) and arginine deiminase (*30*, *31*). The amidinotransferase reaction has been investigated using radiolabeled L-arginine and acid trapping which provided evidence for accumulation of a covalent intermediate after the first half-reaction. The arginine deiminase reaction was studied by similar acid trapping during arginine turnover (*30*) and, more recently, by pre-steady-state kinetics (*31*) and X-ray crystallography (*32*) to characterize the covalent reaction intermediates formed during arginine deiminase catalysis. These two enzymes process different substrates and break a different bond in their substrates, yet they are proposed to proceed through a chemically similar *S*-alkylthiouronium intermediate that is covalently attached to an active site cysteine residue. Apart from these two enzymes, there has been no direct evidence reported that supports a covalent mechanism for other enzymes in this superfamily, including DDAH from any source.

The best structurally characterized DDAH is from *P. aeruginosa* (*Pa* DDAH) for which X-ray crystal structures of the wild-type protein, a product-bound C249S mutant, and a substrate-bound C249S mutant have been reported (*8*). A previous report has shown that this putative DDAH from *P. aeruginosa* hydrolyzes NMMA and ADMA, but not symmetric N^{ω},$N^{\omega'}$-dimethyl-L-arginine, and that arginine is also a very poor substrate (*23*), although k_{cat} or K_M values were not been reported for any substrate and the reaction products were only characterized by a colorimetric assay that employs diacetyl monoxime to derivatize ureido groups formed during the reaction. The physiological substrate for a DDAH enzyme

found in a bacterium that is not known to produce methylated arginines is not well defined, and the colorimetric assay used above is not absolutely specific for citrulline (*16*). Hence, a determination of the actual reaction products and their rate of formation is necessary to avoid misinterpretation. For example, instead of the N^{ω}-nitrogen, the related amidinotransferases use the ornithine side chain as the leaving group (*33*). If *Pa* DDAH actually breaks a similar bond in its NMMA substrate, the resulting reaction products would be ornithine and *N*-methylurea which would be indistinguishable from citrulline when using the colorimetric assay. To rule out this possibility, MALDI-TOF was used to characterize the reaction products after complete hydrolysis of ADMA by purified *Pa* DDAH. The MS analysis identified citrulline and dimethylamine as two new products, unambiguously identifying dimethylamine as the leaving group in the reaction catalyzed by this bacterial enzyme and demonstrating that the products are the same as those found with a mammalian DDAH (*7*).

Once the reaction products had been established, the steady-state kinetic constants for *Pa* DDAH were determined for hydrolysis of a variety of common guanidino-containing compounds by using the diacetyl monoxime derivatization assay (*18*). Asymmetric methylated arginine analogues are shown to be the preferred substrates, supporting the proposition that this enzyme is a true DDAH (Table 1). In fact, the k_{cat}/K_M values for hydrolysis of ADMA and NMMA are both nearly 2-fold higher than those reported for mammalian DDAH isolated from rat kidney (Table 1) (*7*). ADMA is the preferred substrate for *Pa* DDAH (*23*) as reflected in a 1.8-fold increase in k_{cat} and a 2.1-fold decrease in K_M when compared to those of NMMA. It is interesting to note that rat kidney DDAH shows a similar 1.6-fold increase in k_{cat} and a 2.0-fold decrease in K_M when ADMA and NMMA are compared as substrates (*7*). This is a striking similarity considering that these enzymes are only 30% identical in amino acid content and that *P. aeruginosa* is not known to produce any methylated arginine residues. The presence of an N^{ω}-substitution appears to be important for catalysis; N^{ω}-hydroxy-L-arginine and N^{ω}-amino-L-arginine are moderate substrates, but L-arginine is a very poor substrate with a k_{cat}/K_M value 3 orders of magnitude lower than that of ADMA. The relative k_{cat} values of these substrates (ADMA > NMMA $\approx$ N^{ω}-hydroxy-L-arginine > N^{ω}-amino-L-arginine > L-arginine) do not rely solely on either the pK_a of their leaving groups (dimethylamine > methylamine > ammonia > hydrazine > hydroxylamine) or their guanidinium moieties, indicating that factors other than basicity play a role in determining the rate-limiting step during catalysis. Other guanidino compounds commonly found in metabolism are not effectively processed as substrates, further supporting the proposed function of this enzyme as a DDAH. Despite the lack of known methylarginine production in *Pseudomonas* sp., the observation that ADMA is a preferred substrate, and the determination that reaction products and rate constants are comparable to those of a known mammalian DDAH enzyme, are consistent with the assignment of this bacterial enzyme as an authentic DDAH.

In terms of reaction mechanism, accumulation of a covalent intermediate during steady-state turnover has been established for two superfamily members (*28*, *30*, *31*, *33*), but not in others. Our attempts at acid trapping a transient covalent intermediate formed between *Pa* DDAH and NMMA or ADMA during steady-state reactions only resulted in finding a peak with the same mass as the unmodified enzyme as detected by ESI-MS. This observation raised two distinct possibilities.

The first possibility is that, unlike two other superfamily members, *Pa* DDAH does not use a covalent intermediate in its reaction mechanism. Unlike the amidinotransferases, there is no a priori reason for this hydrolase to use covalent catalysis. For example, another guanidino hydrolase, creatine amidinohydrolase, uses a histidine-deprotonated hydroxide as a nucleophile (*34*). Such a difference in mechanism would not be unprecedented; L-histidinol dehydrogenase does not require a cysteine nucleophile, yet many other NAD-linked aldehyde dehydrogenases use a conserved cysteine to form a covalent intermediate (*35*). In fact, the crystal structure of citrulline-bound C249S *Pa* DDAH places a water molecule 3.6 Å from an active site His162 and 3.0 Å from the ureido carbon of a bound product molecule, a distance very similar to the 3.3 Å distance found between the active site C249S's side chain oxygen and the same carbon on the product, clearly allowing the possibility that either Cys249 or this water molecule (after deprotonation by His) could serve as a plausible nucleophile (*8*). Use of a noncovalent mechanism would clearly separate DDAH from other proteins in this superfamily.

The second possibility is that a covalent mechanism is used, but that DDAH does not accumulate an intermediate at detectable levels during steady-state turnover. To test this second possibility, we attempted to increase the rate of intermediate formation through the use of an artificial substrate that replaces the alkylamine leaving group with an activated methane thiol leaving group, SMTC (**3**). Because the pK_a of the *S*-methylthiourea moiety is 9.83 (*36*) and the rest of SMTC is identical in structure to NMMA, this proposed substrate should be very similar in both shape and charge to the natural substrates at the assay pH of 6.2. However, an activated leaving group is expected to increase the formation rate of a covalent intermediate, but should not affect the rate of intermediate decay since the same intermediate would be formed.

Testing of SMTC revealed that it is the best substrate reported for *Pa* DDAH to date, with a 2.7-fold faster k_{cat} and 4.7-fold slower K_M compared to those of its naturally occurring analogue, NMMA (Table 1). The observed increase in k_{cat} does not favor either a covalent or a noncovalent mechanism per se, but does indicate that if hydrolyses of SMTC, ADMA, and NMMA all proceed through the same covalent intermediate, then the decay of this intermediate would not be rate-limiting for either ADMA or NMMA, making SMTC the best candidate for trapping experiments. Reactions of SMTC turnover by *Pa* DDAH were acid quenched at different time points to trap any covalent intermediate that accumulates. Points were taken throughout an entire progress curve at 0, 1, 5, and 30 min to ensure that any observed adduct is transient in nature, and not the result of time-dependent inactivation. In contrast to our results with methylated arginines, ESI-MS of a reaction mixture after turnover for 1 min (Figure 1B) showed the appearance of a new major peak, indicating the formation of a new covalent adduct of 158 $\pm$ 10 Da (Figure 1B). The mass of this adduct is consistent with the expected mass increase (157.09 Da)

after loss of a proton from an amino acid side chain and formation of a covalent bond between *Pa* DDAH and the remaining 1-(iminomethyl)-L-ornithine portion of the SMTC substrate after loss of its methanethiol leaving group. The *Pa* DDAH amino acid sequence contains five cysteine residues as well as other possible nucleophiles, but only one adduct is formed, suggesting that this reaction is specific for a particular residue and not just the result of nonspecific modification. Pre-acidified SMTC does not form a covalent adduct to DDAH, ruling out acid activation of this substrate to a reactive species that can modify protein (Figure 1A). After turnover had proceeded for 5 min, when the rate of DDAH-catalyzed hydrolysis is slowing, probably due to product inhibition (*26*) (Figure 1E), less of the covalent 158 Da adduct is observed (Figure 1C) and more of the unmodified peak is present. Finally, after reaction for 30 min, when total SMTC hydrolysis to citrulline nears completion (Figure 1E) and the rate of DDAH-catalyzed hydrolysis is very slow, the 158 Da covalent adduct is no longer observed (Figure 1D), and the mass spectrum appears to be nearly identical to that of the resting enzyme (Figure 1A). Unrelated to the transient covalent adduct, a constant minor peak resulting from an N-terminal 178 Da adduct is seen at all time points and is due to nonenzymatic α-gluconoylation of the protein during expression (*21*); the ratio of this 178 Da peak to the major peak is constant throughout the entire progress curve, providing further evidence that small differences in the N-terminus do not have significant catalytic consequences.

This series of time points demonstrates that formation of the 158 Da covalent adduct is transient, that the majority of the enzyme carries this covalent adduct during the fastest initial rates, that when less enzyme is saturated by substrate the amount of the adduct declines, and that after the reaction is complete the unmodified enzyme is re-formed. Although there are likely some charge differences between the unmodified enzyme and the transient 158 Da adduct, these differences would be small compared to the overall charge of the protein. So, relative peak heights in the ESI-MS spectrum should be reflective of the amount of unmodified and modified enzyme. These observations are consistent with the proposal that this covalent adduct is a transient intermediate formed during the DDAH catalytic mechanism and not the result of an off-pathway inhibitory alkylation event that would irreversibly proceed over time.

To determine a more exact mass of the observed adduct and to map its point of attachment, the quenched reaction mixture was digested using Glu-C endoproteinase which is active at a low pH where the covalent adduct is also stable. The proteolytic digest was subsequently analyzed by MALDI-TOF, and 24 different peptides were detected, including peptides that contain the active site Cys249, His162, Glu114, and Thr165 residues and most of the other residues found within 6 Å of the ureido group of citrulline bound to *Pa* DDAH (Table 2) (*8*). Of these 24 peptides, only one peptide, the C-terminal $_{240}$YRKIDGGVSCMSLRF$_{254}$, was found both in an unmodified form (*m*/*z* 1733) and with an additional mass increase (*m*/*z* 1890) corresponding to a 157.3 ± 0.4 Da adduct which matches that calculated for the proposed covalent intermediate (157.09 Da). The *m*/*z* 1890 peptide underwent a dominant fragmentation involving neutral loss of 157 and 190 Da to produce *m*/*z* 1733 and 1700 fragments,

Scheme 1

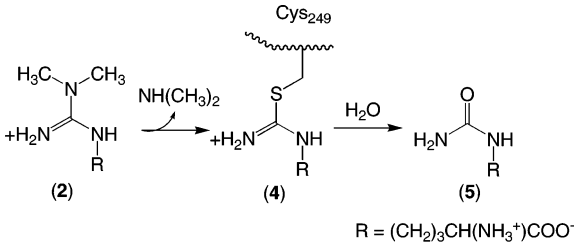

respectively. These ion peaks represent loss of the covalent adduct, fragmenting on either side of a sulfur atom, thereby implicating the one cysteine residue in this peptide, Cys249, as the point of attachment. In addition, the peptide at *m*/*z* 1890 is not seen in the MALDI reflectron spectrum, demonstrating that it contains a bond that readily fragments after ionization, as would be expected for a sulfide−carbamide bond. The immonium ions, b ions, and y ions for the adducted peptide are similar to those of the unmodified peptide, confirming that the same peptide sequence is involved in both cases. The adducted peptide PSD shows modified y_{10}* ions that appear as a pair of peaks separated by 34 Da. They represent dual fragmentation products with both backbone fragmentation and loss of the unstable adduct, again fragmenting on either side of the sulfide bond and implicating Cys249 as the point of attachment (Figure 2).

To verify the importance of Cys249 in the mechanism, a conservative mutation to a serine residue was introduced at this position. The crystal structure of a C249S *Pa* DDAH has already been reported and shows that this mutant is still capable of proper folding and can correctly bind an ADMA substrate (*8*). The C249S mutant does not hydrolyze ADMA (*8*), NMMA, or the activated substrate SMTC. Quenched reaction mixtures of C249S and SMTC show one major peak by ESI-MS, matching that of the unmodified mutant enzyme. No evidence for either productive turnover or nonproductive accumulation of a covalent adduct was observed for the C249S mutant, presumably because the increased pK_a of the mutant serine side chain prevents it from acting as an effective nucleophile.

These results are consistent with a proposed covalent mechanism for DDAH catalysis that uses Cys249 as an active site nucleophile and proceeds through a covalent *S*-alkylthiouronium intermediate (**4**) that can be subsequently hydrolyzed to yield citrulline (**5**) (Scheme 1). Presumably, formation and decay of the intermediate (**4**) detected here proceed through tetrahedral adducts formed by attack of a nucleophile, Cys249 and hydroxide, respectively. Recent crystal structures have shown examples of tetrahedral and *S*-alkylthiouronium intermediates during catalysis by another superfamily member, arginine deiminase (*32*). In the case of SMTC and *Pa* DDAH, the decay of the intermediate must be at least partially rate limiting for this transient adduct to be detectable during steady-state reactions. Further characterization will be required to rigorously define the rate-limiting steps during hydrolysis of each substrate and to determine whether they proceed through the same mechanism.

The observation that SMTC is a good substrate is also significant because this compound is often used for •NO synthase inhibition studies (*37*). Our observations with *Pa* DDAH suggest that SMTC might achieve part of its

physiological effects by competing for binding to DDAH and inhibiting the hydrolysis of endogenous methylated arginines, and also that •NO synthase inhibition by SMTC might ultimately be limited by its DDAH-catalyzed hydrolysis to citrulline. Therefore, future design of selective inhibitors of •NO synthesis should consider the interaction of these compounds with •NO synthase isoforms and with DDAH isoforms as well.

Although the roles of mammalian DDAH isozymes are becoming better understood (*4*), it is still unclear what advantage a DDAH could impart to a bacterium that is not known to produce methylated arginines. Production of a bacterial DDAH could be a response to environmental substrates and might be used to catabolize ADMA to prevent toxicity of this compound or to provide citrulline for further use by the bacterium. In fact, *P. aeruginosa* is commonly found in urinary tract infections (*38*), and human urine contains higher concentrations of ADMA than L-arginine (*39*). Also, a bacterial DDAH could potentially upset the normal regulation of host •NO production. One report suggests that •NO may mediate epithelial damage during *P. aeruginosa* infections of human respiratory tissue, and that an increase in the level of endogenous ADMA can limit this effect (*40*); therefore, bacterial DDAH could possibly play a role in the etiology of lung damage caused by this organism. It is interesting to note that in addition to *P. aeruginosa*, putative DDAH sequences have also been identified in other lung pathogens, including *Legionella pneumophila* and *Mycobacterium tuberculosis*. Intriguingly, all of these organisms have downstream ORFs encoding putative proteins involved in amino acid transport. However, no knockouts have yet been reported to test whether bacterial DDAH isozymes are virulence factors in these lung pathogens.

DDAH is part of a larger superfamily of enzymes that catalyze the modification of guanidino groups (*13*); many of these enzymes are potential drug targets. These enzymes can show considerable diversity (*13*). For example, the amidinotransferases use arginine as a substrate and transfer the terminal amidino group to a different amine, yielding ornithine as one product. However, the arginine deiminases break a different bond of the guanidino group when catalyzing the hydrolysis of arginine to citrulline and ammonia. Despite their differences, these two enzymes have been shown to utilize a covalent intermediate bound to an active site cysteine residue (*13*). In contrast to these previous findings, our initial tests with the natural substrates of DDAH did not indicate any intermediate formation, suggesting that an alternative mechanism might be used by this hydrolytic enzyme. However, use of a substrate with an activated leaving group allowed us to trap and characterize a transient covalent adduct that forms during turnover. This adduct is chemically similar to the reaction intermediates characterized in two other superfamily members and strongly supports the proposal that DDAH as well as the rest of this superfamily may all use an *S*-alkylthiouronium covalent intermediate in their catalytic mechanisms.

In summary, these results provide strong evidence supporting the transient accumulation of a covalent intermediate during hydrolysis of *S*-methyl-L-thiocitrulline (SMTC) by DDAH and also identify the active site Cys249 residue as the catalytic nucleophile required for intermediate formation. The use of covalent catalysis by DDAH further unifies this superfamily of enzymes and suggests that an *S*-alkylthiouronium intermediate may be a universal feature in their mechanisms.

REFERENCES

1. Vallance, P., and Leiper, J. (2002) Blocking NO synthesis: How, where and why? *Nat. Rev. Drug Discovery 1*, 939−950.
2. Floyd, R. A. (1999) Antioxidants, oxidative stress, and degenerative neurological disorders, *Proc. Soc. Exp. Biol. Med. 222*, 236−245.
3. Thomsen, L. L., and Miles, D. W. (1998) Role of nitric oxide in tumour progression: Lessons from human tumours, *Cancer Metastasis Rev. 17*, 107−118.
4. Dayoub, H., Achan, V., Adimoolam, S., Jacobi, J., Stuehlinger, M. C., Wang, B. Y., Tsao, P. S., Kimoto, M., Vallance, P., Patterson, A. J., and Cooke, J. P. (2003) Dimethylarginine dimethylaminohydrolase regulates nitric oxide synthesis: Genetic and physiological evidence, *Circulation 108*, 3042−3047.
5. MacAllister, R. J., Parry, H., Kimoto, M., Ogawa, T., Russell, R. J., Hodson, H., Whitley, G. S., and Vallance, P. (1996) Regulation of nitric oxide synthesis by dimethylarginine dimethylaminohydrolase, *Br. J. Pharmacol. 119*, 1533−1540.
6. Leiper, J., and Vallance, P. (1999) Biological significance of endogenous methylarginines that inhibit nitric oxide synthases, *Cardiovasc. Res. 43*, 542−548.
7. Ogawa, T., Kimoto, M., and Sasaoka, K. (1989) Purification and properties of a new enzyme, N^G,N^G-dimethylarginine dimethylaminohydrolase, from rat kidney, *J. Biol. Chem. 264*, 10205−10209.
8. Murray-Rust, J., Leiper, J., McAlister, M., Phelan, J., Tilley, S., Santa Maria, J., Vallance, P., and McDonald, N. (2001) Structural insights into the hydrolysis of cellular nitric oxide synthase inhibitors by dimethylarginine dimethylaminohydrolase, *Nat. Struct. Biol. 8*, 679−683.
9. Leiper, J., Murray-Rust, J., McDonald, N., and Vallance, P. (2002) *S*-Nitrosylation of dimethylarginine dimethylaminohydrolase regulates enzyme activity: Further interactions between nitric oxide synthase and dimethylarginine dimethylaminohydrolase, *Proc. Natl. Acad. Sci. U.S.A. 99*, 13527−13532.
10. Knipp, M., Braun, O., Gehrig, P. M., Sack, R., and Vasak, M. (2003) Zn(II)-free dimethylargininase-1 (DDAH-1) is inhibited upon specific Cys-*S*-nitrosylation, *J. Biol. Chem. 278*, 3410−3416.
11. Bogumil, R., Knipp, M., Fundel, S. M., and Vasak, M. (1998) Characterization of dimethylargininase from bovine brain: Evidence for a zinc binding site, *Biochemistry 37*, 4791−4798.
12. Leiper, J. M., Santa Maria, J., Chubb, A., MacAllister, R. J., Charles, I. G., Whitley, G. S., and Vallance, P. (1999) Identification of two human dimethylarginine dimethylaminohydrolases with distinct tissue distributions and homology with microbial arginine deiminases, *Biochem. J. 343* (Part 1), 209−214.
13. Shirai, H., Blundell, T. L., and Mizuguchi, K. (2001) A novel superfamily of enzymes that catalyze the modification of guanidino groups, *Trends Biochem. Sci. 26*, 465−468.
14. Gill, S. C., and von Hippel, P. H. (1989) Calculation of protein extinction coefficients from amino acid sequence data, *Anal. Biochem. 182*, 319−326.
15. Boyde, T. R., and Rahmatullah, M. (1980) Optimization of conditions for the colorimetric determination of citrulline, using diacetyl monoxime, *Anal. Biochem. 107*, 424−431.
16. Veniamin, M. P., and Vakirtzi-Lemonias, C. (1970) Chemical basis of the carbamidodiacetyl micromethod for estimation of urea, citrulline, and carbamyl derivatives, *Clin. Chem. 16*, 3−6.
17. Person, M. D., Monks, T. J., and Lau, S. S. (2003) An integrated approach to identifying chemically induced posttranslational modifications using comparative MALDI-MS and targeted HPLC-ESI-MS/MS, *Chem. Res. Toxicol. 16*, 598−608.
18. Knipp, M., and Vasak, M. (2000) A colorimetric 96-well microtiter plate assay for the determination of enzymatically formed citrulline, *Anal. Biochem. 286*, 257−264.
19. Wang, S. C., Person, M. D., Johnson, W. H., Jr., and Whitman, C. P. (2003) Reactions of *trans*-3-chloroacrylic acid dehalogenase with acetylene substrates: Consequences of and evidence for a hydration reaction, *Biochemistry 42*, 8762−8773.
20. Clauser, K. R., Baker, P., and Burlingame, A. L. (1999) Role of accurate mass measurement (±10 ppm) in protein identification

strategies employing MS or MS/MS and database searching, *Anal. Chem. 71*, 2871−2882.
21. Geoghegan, K. F., Dixon, H. B., Rosner, P. J., Hoth, L. R., Lanzetti, A. J., Borzilleri, K. A., Marr, E. S., Pezzullo, L. H., Martin, L. B., LeMotte, P. K., McColl, A. S., Kamath, A. V., and Stroh, J. G. (1999) Spontaneous α-*N*-6-phosphogluconoylation of a "His tag" in *Escherichia coli*: The cause of extra mass of 258 or 178 Da in fusion proteins, *Anal. Biochem. 267*, 169−184.
22. Plevin, M. J., Magalhaes, B. S., Harris, R., Sankar, A., Perkins, S. J., and Driscoll, P. C. (2004) Characterization and manipulation of the *Pseudomonas aeruginosa* dimethylarginine dimethylaminohydrolase monomer−dimer equilibrium, *J. Mol. Biol. 341*, 171−184.
23. Santa Maria, J., Vallance, P., Charles, I. G., and Leiper, J. M. (1999) Identification of microbial dimethylarginine dimethylaminohydrolase enzymes, *Mol. Microbiol. 33*, 1278−1279.
24. Kimoto, M., Miyatake, S., Sasagawa, T., Yamashita, H., Okita, M., Oka, T., Ogawa, T., and Tsuji, H. (1998) Purification, cDNA cloning and expression of human N^G,N^G-dimethylarginine dimethylaminohydrolase, *Eur. J. Biochem. 258*, 863−868.
25. Knipp, M., Charnock, J. M., Garner, C. D., and Vasak, M. (2001) Structural and functional characterization of the Zn(II) site in dimethylargininase-1 (DDAH-1) from bovine brain. Zn(II) release activates DDAH-1, *J. Biol. Chem. 276*, 40449−40456.
26. Stone, E. M., and Fast, W. (2005) A continuous spectrophotometric assay for dimethylarginine dimethylaminohydrolase activity, *Anal. Biochem.*, submitted for review.
27. Biemann, K. (1990) Appendix 5. Nomenclature for peptide fragment ions (positive ions), *Methods Enzymol. 193*, 886−887.
28. Grazi, E., and Rossi, N. (1968) Transamidinase of hog kidney. VII. Cysteine at the amidine-binding site, *J. Biol. Chem. 243*, 538−542.
29. Humm, A., Fritsche, E., Steinbacher, S., and Huber, R. (1997) Crystal structure and mechanism of human L-arginine:glycine amidinotransferase: A mitochondrial enzyme involved in creatine biosynthesis, *EMBO J. 16*, 3373−3385.
30. Smith, D. W., and Fahrney, D. E. (1978) Catalysis by arginine deiminase: Evidence for a covalent intermediate, *Biochem. Biophys. Res. Commun. 83*, 101−106.
31. Lu, X., Galkin, A., Herzberg, O., and Dunaway-Mariano, D. (2004) Arginine deiminase uses an active-site cysteine in nucleophilic catalysis of L-arginine hydrolysis, *J. Am. Chem. Soc. 126*, 5374−5375.
32. Das, K., Butler, G. H., Kwiatkowski, V., Clark, A. D., Jr., Yadav, P., and Arnold, E. (2004) Crystal structures of arginine deiminase with covalent reaction intermediates: Implications for catalytic mechanism, *Structure 12*, 657−667.
33. Humm, A., Fritsche, E., Mann, K., Gohl, M., and Huber, R. (1997) Recombinant expression and isolation of human L-arginine:glycine amidinotransferase and identification of its active-site cysteine residue, *Biochem. J. 322* (Part 3), 771−776.
34. Coll, M., Knof, S. H., Ohga, Y., Messerschmidt, A., Huber, R., Moellering, H., Russmann, L., and Schumacher, G. (1990) Enzymatic mechanism of creatine amidinohydrolase as deduced from crystal structures, *J. Mol. Biol. 214*, 597−610.
35. Teng, H., Segura, E., and Grubmeyer, C. (1993) Conserved cysteine residues of histidinol dehydrogenase are not involved in catalysis. Novel chemistry required for enzymatic aldehyde oxidation, *J. Biol. Chem. 268*, 14182−14188.
36. Jencks, W. P., and Regenstein, J. (1968) in *Handbook of Biochemistry* (Sober, H. A., Ed.) pp J-148−J-189, CRC Press, Cleveland, OH.
37. Narayanan, K., and Griffith, O. W. (1994) Synthesis of L-thiocitrulline, L-homothiocitrulline, and *S*-methyl-L-thiocitrulline: A new class of potent nitric oxide synthase inhibitors, *J. Med. Chem. 37*, 885−887.
38. Nicolle, L. E. (2002) Resistant pathogens in urinary tract infections, *J. Am. Geriatr. Soc. 50*, S230−S235.
39. Kakimoto, Y., and Akazawa, S. (1970) Isolation and identification of N^G,N^G- and N^G,N'^G-dimethyl-arginine, *N*-ε-mono-, di-, and trimethyllysine, and glucosylgalactosyl- and galactosyl-δ-hydroxylysine from human urine, *J. Biol. Chem. 245*, 5751−5758.
40. Dowling, R. B., Newton, R., Robichaud, A., Cole, P. J., Barnes, P. J., and Wilson, R. (1998) Effect of inhibition of nitric oxide synthase on *Pseudomonas aeruginosa* infection of respiratory mucosa in vitro, *Am. J. Respir. Cell Mol. Biol. 19*, 950−958.

BI047407R